RESEARCH ARTICLE

DOI: 10.34256/famr2415

Frontiers in Advanced Materials Research

Utilizing Chlorophyll as a Natural Chelating Agent for the Remediation of Heavy Metal Pollution: A Density Functional Theory Study

C. Pitchumani Violet Mary [a,*], S. Shalini Packiam Kamala [b]

[a] Department of Physics, Sri Shakthi Institute of Engineering and Technology, Coimbatore 641 062, India

[b] Michael Job College of Arts and Science for Women, Coimbatore 641 046, India

* Corresponding Author: mviolet88@gmail.com

Received: 01-03-2024, Revised: 27-04-2024, Accepted: 07-05-2024, Published: 15-05-2024

Abstract: Heavy metal pollution, driven by industrialization, urbanization, and inadequate waste management, poses significant environmental and health risks. Toxic elements such as lead (Pb), mercury (Hg), cadmium (Cd), and arsenic (As) persist in ecosystems and bioaccumulate within biological systems, leading to severe health effects. Major contamination sources include industrial processes, agricultural practices, and improper waste disposal. Unlike organic pollutants, heavy metals do not degrade over time, allowing long-distance transport and deposition in soils and sediments. Traditional remediation methods often generate secondary waste, while adsorption techniques face material regeneration challenges. Natural chelating agents like chlorophyll, integral to photosynthesis, offer a promising alternative due to their ability to form stable complexes with heavy metals, reducing their bioavailability and toxicity. This study explores chlorophyll's potential in sequestering heavy metals through Density Functional Theory (DFT) to analyze the electronic structure and bonding characteristics of metal-chlorophyll complexes, aiming to develop sustainable and eco-friendly remediation strategies.

Keywords: Heavy metal pollution, Chlorophyll, Eco-friendly remediation, Waste management, Density Functional Theory (DFT), Metal-chlorophyll complexes

1. Introduction

Heavy metal pollution is a growing environmental problem driven by rapid industrialization, urbanization, and inadequate waste management. Elements such as lead (Pb), mercury (Hg), cadmium (Cd), and arsenic (As) are particularly problematic due to their high toxicity, persistence, and propensity to bioaccumulate within biological systems [1]. While some heavy metals, like zinc (Zn) and copper (Cu), are essential in trace amounts for biological functions, others have no known beneficial role and are detrimental even at low concentrations

[2, 3]. Major sources of heavy metal contamination include industrial processes (such as mining, smelting, and manufacturing), agricultural practices (notably the use of pesticides and fertilizers), and improper waste disposal methods (including electronic waste and sewage sludge) [4-6].

The persistence and toxicity of heavy metals in the environment pose significant risks. Unlike organic pollutants, heavy metals do not degrade over time and can remain in ecosystems indefinitely. They are capable of long-distance transport via air and water, ultimately depositing in soils and sediments. Within biological systems, heavy metals can accumulate in tissues and organs, leading to chronic health effects. For instance, lead exposure is linked to cognitive impairments and developmental delays in children, while mercury exposure can cause severe neurological damage and kidney dysfunction [7-12].

Given these serious implications, there is an urgent need for effective remediation strategies. Traditional methods, such as chemical precipitation and ion exchange, typically involve adding chemicals to convert soluble heavy metals into insoluble forms that can be separated from the aqueous phase. While these methods can be effective, they often generate secondary waste requiring further treatment and disposal. Adsorption techniques, using materials like activated carbon or biochar, can remove heavy metals from water effectively, but the regeneration and disposal of these adsorbent materials present additional challenges [13].

In this context, the use of natural chelating agents offers a promising alternative. Chelating agents are compounds that form multiple bonds with a single metal ion, creating a stable complex. This process, known as chelation, effectively immobilizes heavy metals, reducing their bioavailability and toxicity. Natural chelating agents, such as phytochelatins, humic acids, and chlorophyll, are biodegradable, environmentally friendly, and often more cost-effective compared to synthetic chelators [14].

Chlorophyll, the pigment responsible for the green colour of plants and algae, is integral to the process of photosynthesis. It captures light energy and converts it into chemical energy, facilitating the production of organic molecules from carbon dioxide and water. The structure of chlorophyll comprises a porphyrin ring with a central magnesium ion, crucial for its light-absorbing properties [15].

The porphyrin ring in chlorophyll, a key component of the photosynthetic machinery, is composed of four nitrogen-containing pyrrole rings connected by carbon bridges. This unique structure provides multiple binding sites for metal ions, making chlorophyll an effective chelating agent. The central magnesium ion in the porphyrin ring can be replaced by other metal ions, such as lead, mercury, and cadmium, through a process known as metal exchange. The formation of these stable metal-chlorophyll complexes can have significant environmental implications, as they can be more readily removed from the environment compared to the free metal ions.

The ability of porphyrins to chelate a wide range of metal ions is well-documented. This property is attributed to the delocalized π-electrons within the tetrapyrollic skeleton, which allows for the coordination of various metal species. The extensive research on metalloporphyrins has demonstrated that dozens of elements from the periodic table can be chelated into the center of the macrocycle.

The metal-exchange process in chlorophyll is particularly important, as it can result in the formation of stable complexes with heavy metals like lead, mercury, and cadmium. These metal-chlorophyll complexes can be more readily removed from the environment compared to the free metal ions, potentially mitigating the environmental impact of heavy metal contamination [16-18].

This research article aims to investigate the feasibility and effectiveness of chlorophyll as a natural chelating agent for the removal of heavy metals. The study will explore the mechanisms underlying chlorophyll's interaction with various heavy metal ions, evaluate its binding efficiency, and assess its potential applications in environmental remediation. By employing Density Functional Theory (DFT) studies, we aim to gain detailed insights into the electronic structure and bonding characteristics of metal-chlorophyll complexes. The research includes analysis of interaction energies, charge transfer phenomena, and topological properties to verify the detoxification capabilities of chlorophyll. This study specifically addresses chlorophyll's chelating properties across a spectrum of heavy metal ions, including Ag^{1+}, Ag^{2+}, Ag^{3+}, As^{5+}, Cd^{2+}, Cr^{4+}, Cr^{5+}, Cr^{6+}, Hg^{2+}, Pb^{2+}, Pb^{4+}, Se^{6+}, and Tl^{3+}, utilizing density functional theory methods. Through this investigation, we aim to elucidate the mechanisms by which chlorophyll effectively sequesters heavy metals, contributing to the development of sustainable solutions for environmental pollution control.

2. Computational details

Density functional theory method was employed to study the chelation of heavy metal ions by the chlorophyll. The metal-free chlorophyll and its metal complexes were optimized using B3LYP functional which includes Becke's three (B3) parameter exchange functional [19] along with Lee, Yang, Parr's (LYP) gradient corrected correlation functional [20] along with the mixed basis set 6-311g(d)+LANL2DZ (6-311g(d) for non-metal atoms and LANL2DZ for metal ions) [21-23]. Harmonic –vibrational-frequency analysis has been carried out at the same computational levels and the absence of imaginary frequencies confirms that the structures are at energetic minima on PES. The interaction energy has been corrected for BSSE using the counterpoise procedure (CP) of Boys and Bernadi [24] using the following equation.

$$E_{int}(AB) = E_{AB}(AB) - E_{AB}(A) - E_{AB}(B) \quad (1)$$

where $E_{AB}(AB)$ is the energy of the complex, $E_{AB}(A)$is the energy of the isolated A and $E_{AB}(B)$ is the energy of the isolated B. The MIA is one of the intuitive tool to study the affinity

of the metal ions towards the chelating agent and their corresponding values are computed as the negative of the enthalpy variation for the dissociation process of the CHL-M^{n+} reactions and it has been calculated as,

$$MIA = -[E_{el}(BM) - E_{el}(B) - E_{el}(M) + (E_{vib}(BM) - E_{vib}(B))] \quad (2)$$

where E_{el} is the electronic energy obtained from the SCF computation and E_{vib} includes the zero point energy and temperature corrections from 0 to 298 K obtained by the thermo-chemical analysis of vibrational frequencies [25-27]. The individual atomic charges and details about the orbitals involved in the charge transfer interactions between metal ions and the donor ligand atoms were obtained using the NPA [28] and NBO [29] analyses. The topological properties such as electron density $\rho(r)$, Laplacian of electron density $\nabla^2\rho(r)$, and total electron density $H_{BCP}(r)$ at the BCP corresponding to the coordination bonds of the CHL-M^{n+} complexes have been calculated using the Bader's QTAIM theory [30]. Wavefunction files were generated from the Gaussian output files at the B3LYP/6-311g(d)+LANL2DZ level of theory to perform AIM calculations and the topological parameters were obtained using Multiwfn_3.3.7 software [31]. All the calculations were carried out using the Gaussian 09 software [32].

3. Results and discussion

3.1 Geometrical parameter

The optimized geometries of the isolated CHL and CHL-M^{n+} metal complexes are shown in Figure 1 and the obtained metal coordination parameters are presented in Table 1. In the CHL-Ag^{2+}, CHL-Cr^{4+}, CHL- Cr^{5+}, CHL- Cr^{6+}, and CHL-Se^{6+} complexes, all the ligand atoms, and metal ions are in the same plane and exhibits nearly square planar geometry with little deviations of about ± 0.20 to 3.00 Å. Whereas, in the CHL-Ag^{1+}, CHL-Ag^{3+}, CHL-As^{5+}, CHL-Cd^{2+}, CHL-Hg^{2+}, CHL-Pb^{2+}, CHL-Pb^{4+}, and CHL-Tl^{3+} complexes the structure losses its planarity due to the disposition of the central metal ion that is situated out of plane (which looks like square pyramidal) with respect to the coordinating ligand atoms and the degree of deviation from the planarity is about ± 0.40 to 78.70 Å. The average N-M^{n+} coordination distance of the CHL-M^{n+} complexes is found to be in the range of 2.03 to 2.64 Å. Among the various CHL-M^{n+} complexes, the Pb^{2+}, Pb^{4+}, and Tl^{3+} interacted CHL complexes show the maximum N-M^{n+} coordination distances of about 2.38, 2.40 and 2.64 Å respectively and this may due to the larger ionic radii and atomic size of Pb and Tl metals. Whereas the Cr^{4+}, Cr^{5+}, and Cr^{6+} interacted complexes show the minimum N-M^{n+} coordination distances of about 2.04, 2.05, and 2.03 Å and this may be due to the smallest atomic size and ionic radii of the Cr metal. For the Ag^{1+}, Ag^{2+}, $Ag3^{+}$, As^{5+}, Cd^{2+}, Hg^{2+}, and Se^{6+} interacted complexes, the average N-M^{n+} coordination distance is found to be intermediate in the range of 2.08 to 2.30Å. It is noteworthy that, larger the atomic size and ionic radii results in larger coordination distance and smaller the atomic size and ionic radii results in smaller coordination distance. In the case of metal ions with smaller ionic radii and larger atomic size or vice-versa, the coordination distance will be in the intermediate range.

Thus, atomic size, ionic radii and oxidation states of the metal ions strongly influence the metal-ligand coordination distances.

Table 1. Coordination parameters (bond lengths in Å, bond angles in degrees) of the CHL-Mn+ metal complexes calculated at B3LYP/6-311g(d)+LANL2DZ level of theory

Complexes	N6-M^{n+}	N7-M^{n+}	N8-M^{n+}	N9-M^{n+}	N6-M^{n+}-N7	N6-M^{n+}-N8	N6-M^{n+}-N9	N7-M^{n+}-N8	N7-M^{n+}-N9	N8-M^{n+}-N9
CHL-Ag^{1+}	2.24	2.4	2.23	2.35	83.3	139.3	79.8	84.8	137.8	83.4
CHL-Ag^{2+}	2.07	2.19	2.08	2.13	90.2	178.1	87	91.7	177.1	91.2
CHL-Ag^{3+}	2.05	2.14	2.07	2.09	90.4	173.5	87.8	91.5	171.8	91.3
CHL-As^{5+}	2.05	2.39	2.09	2.03	81.08	137.2	85	82.86	146.12	86.8
CHL-Cd^{2+}	2.14	2.26	2.15	2.21	88.2	159.6	84.9	89.7	157.7	89.4
CHL-Cr^{4+}	2	2.11	2.02	2.03	89.9	178.3	87.5	91.5	177.3	91
CHL-Cr^{6+}	2	2.14	2.03	2.04	89.9	178.2	87.6	91.6	177.3	91
CHL-Cr^{6+}	1.98	2.12	2	2	88.5	177	89	92.3	177.4	90.2
CHL-Hg^{2+}	2.23	2.36	2.23	2.3	84.4	144	81.5	85.6	142.2	85.6
CHL-Pb^{2+}	2.31	2.52	2.34	2.35	76	120.2	75.4	76.9	125	78.4
CHL-Pb^{4+}	2.36	2.53	2.33	2.37	74.9	116.7	73.4	76.5	123	77.4
CHL-Se^{6+}	2.07	2.3	2.11	2.03	88.7	177.4	88.9	90.9	175.7	91.4
CHL-Tl^{3+}	2.6	2.75	2.57	2.63	68	101.3	65.3	69.2	107.3	69.4

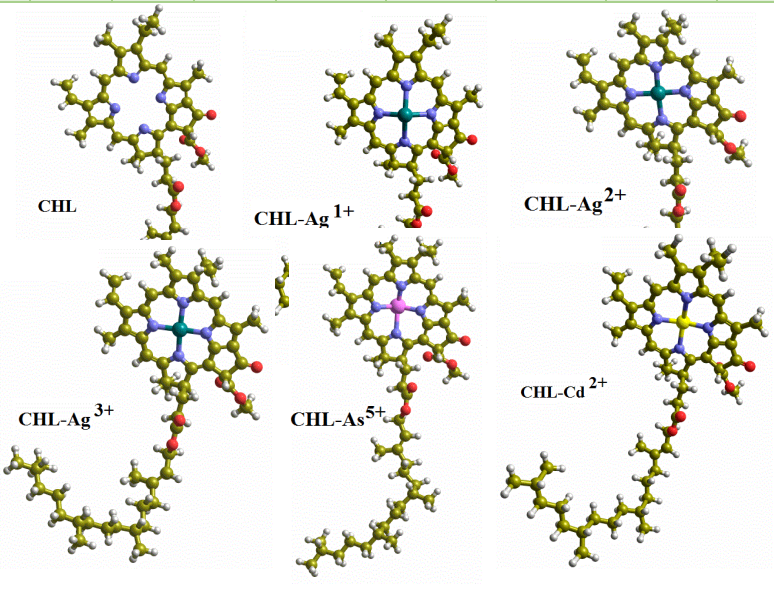

Figure 1 Cont

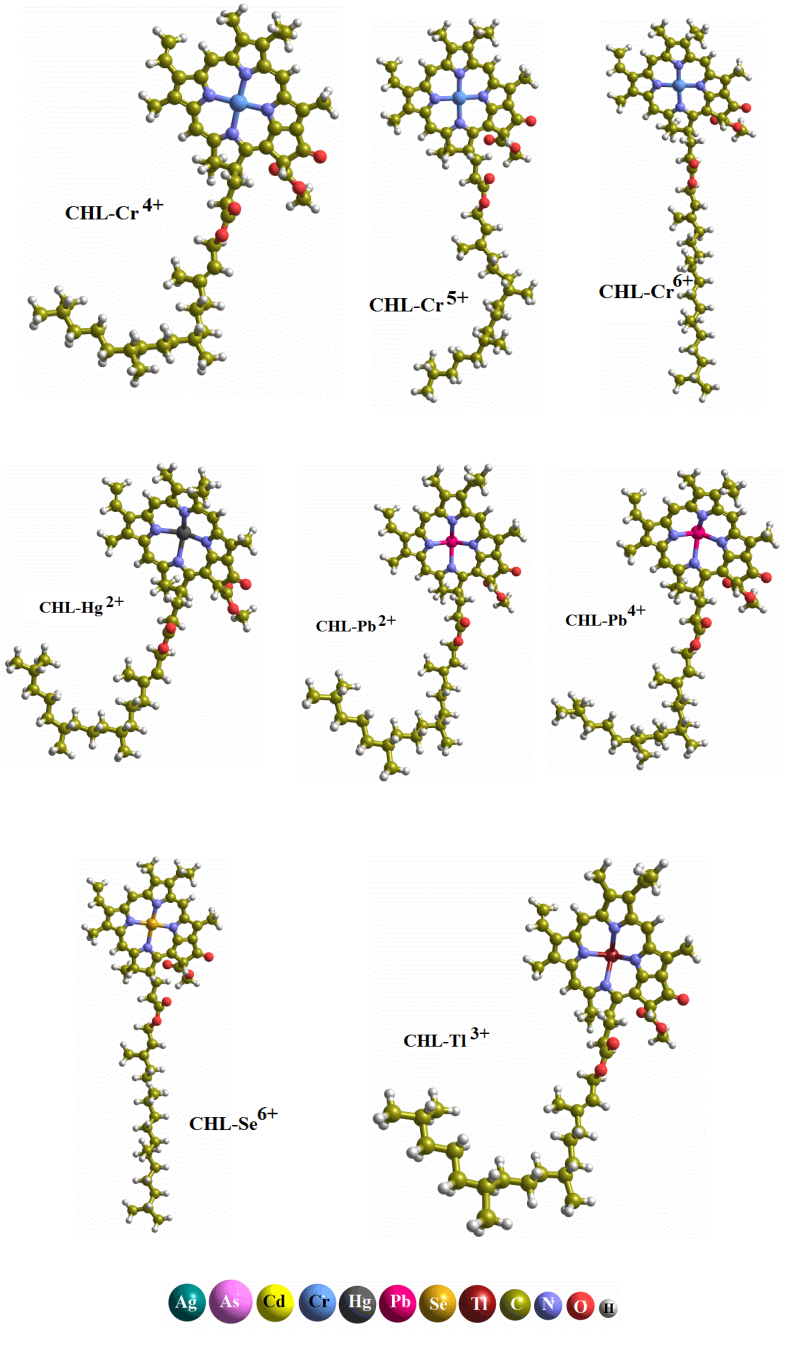

Figure 1. Optimized geometries of CHL-Mn+ (where M = Ag, As, Cd, Cr, Hg, Pb, Se, and Tl; n=1, 2, 3, 4, 5, and 6) metal complexes at B3LYP/6-311g (d)+LANL2DZ level of theory.

3.2 Interaction energy and Metal Ion affinity

The ideal chelator should possess a high affinity towards the toxic metals. Hence, in order to study the stability of the interaction and the affinity of the various metal ions towards the chelator, the interaction energy, and metal ion affinity was calculated using the equations 1 and 2 at B3LYP/6-311g (d) +LANL2DZ level of theory and the results are tabulated in Table 2. As can see from the Table 2, the interaction energy calculated for all the CHL-M^{2+} metal complexes are found to be negative, which implies that the interaction between the metal ions and the chlorophyll are exothermic in nature. The calculated interaction energy and MIA of the CHL-M^{n+} (where M = Ag, As, Cd, Cr, Hg, Pb, Se and Tl; n= 1, 2, 3, 4, 5, and 6) metal complexes are -268.04 and 258.59, -735.14 and 719.74, -1381.95 and 1358.37, -3297.42 and 3262.69, -633.38 and 617.07, -2258.39 and 2236.16, -3729 and 3703.56, -5633.46 and 5587.57, -625.05 and 608.28, -587.07 and 572.01, -1919.95 and 1891.37, -4933.71 and 4883.49, -1154.04 and 1126.53kcal/mol respective of CHL-Ag^{1+}, CHL-Ag^{2+}, CHL-Ag^{3+}, CHL-As^{5+}, CHL-Cd^{2+}, CHL-Cr^{4+}, CHL- Cr^{5+}, CHL- Cr^{6+}, CHL-Hg^{2+}, CHL-Pb^{2+}, CHL-Pb^{4+}, CHL-Se^{6+}, and CHL-Tl^{3+} metal complexes respectively. The interaction energy and MIA values of CHL-M^{n+} complexes in the present study follow the order: CHL-Cr^{6+}>CHL-Se^{6+}>CHL-Cr^{5+}>CHL-As^{5+}>CHL-Cr^{4+}>CHL-Pb^{4+}>CHL-Ag^{3+}>CHL-Tl^{3+}>CHL-Ag^{2+}>CHL-Cd^{2+}> CHL-Hg^{2+}>CHL-Pb^{2+}>CHL-Ag^{1+} respectively. From the obtained results, it is noteworthy that the oxidation states and atomic size of the metal ions significantly influence the interaction energy and MIA of the CHL-M^{n+} complexes. The metal ions with oxidation state 6+ such as Cr^{6+} and Se^{6+} interacted metal complexes possess the highest interaction energy and MIA and the ionic radii of Cr^{6+} and Se^{6+} is 0.26 and 0.28 Å.

Table 2 Interaction energies and MIA (in kcal/mol) of the CHL-Mn+ metal complexes calculated at B3LYP/6-311g (d)+LANL2DZ level of theory and Ionic radii (in Å) of the metal ions.

Complexes	IE	MIA	Ionic radii
CHL-Ag^{1+}	-268.04	258.59	1.00
CHL-Ag^{2+}	-735.14	719.74	0.79
CHL-Ag^{3+}	-1381.95	1358.37	0.67
CHL-As^{5+}	-3297.42	3262.69	0.34
CHL-Cd^{2+}	-633.38	617.07	0.78
CHL-Cr^{4+}	-2258.39	2236.16	0.41
CHL-Cr^{5+}	-3729	3703.56	0.35
CHL-Cr^{6+}	-5633.46	5587.57	0.26
CHL-Hg^{2+}	-625.05	608.28	0.96
CHL-Pb^{2+}	-587.07	572.01	0.98
CHL-Pb^{4+}	-1919.95	1891.37	0.65
CHL-Se^{6+}	-4933.71	4883.49	0.28
CHL-Tl^{3+}	-1154.04	1126.53	0.75

Whereas the metal ions with oxidation state 1+ such as Ag^{1+} possess the least interaction energy and MIA, and the ionic radii of Ag^{1+} are 1.00 Å. This implies that the interaction energy and MIA were found to be increased as the oxidation states of the metal ions increases from 1+ to 6+ and decreases when the atomic size of the metal ions increases. The reason for the change in interaction energy with respect to the oxidation state is that the charge accepting ability of the metal ions increases as there is an increase in their oxidation states, which in turn enhance the interaction between the metal ions and the chelator resulting in highest interaction energy.

Table 3. Natural atomic charges (in e) of the CHL-Mn+ metal complexes calculated at B3LYP/6-311g (d)+LANL2DZ level of theory and Ionic radii (in Å) of the metal ions.

Complexes	N6	N7	N8	N9	M^{n+}
CHL	-0.46	-0.43	-0.47	-0.44	-
CHL-Ag^{1+}	-0.58	-0.53	-0.59	-0.55	0.61
CHL-Ag^{2+}	-0.56	-0.54	-0.58	-0.54	0.89
CHL-Ag^{3+}	-0.52	-0.56	-0.54	-0.54	0.98
CHL-As^{5+}	-0.69	-0.57	-0.69	-0.71	1.58
CHL-Cd^{2+}	-0.69	-0.64	-0.70	-0.67	1.45
CHL-Cr^{4+}	-0.60	-0.58	-0.60	-0.59	0.99
CHL-Cr^{5+}	-0.56	-0.54	-0.61	-0.59	1.05
CHL-Cr^{6+}	-0.60	-0.56	-0.59	-0.57	0.99
CHL-Hg^{2+}	-0.67	-0.62	-0.68	-0.65	1.38
CHL-Pb^{2+}	-0.69	-0.61	-0.69	-0.68	1.41
CHL-Pb^{4+}	-0.65	-0.60	-0.71	-0.68	1.49
CHL-Se^{6+}	-0.54	-0.50	-0.56	-0.55	1.08
CHL-Tl^{3+}	-0.55	-0.52	-0.60	-0.57	0.92

3.3 NPA analysis

During the formation of CHL-M^{n+} complexes, there may be a transfer of charges from the coordinating nitrogen atoms such as N6, N7, N8, and N9 to the metal ions. The amount of charge transferred from the coordinating atoms to the metal ions during complexation can be identified by finding the difference between the charge of metal ion before and after complexation. Hence, in order to find out the individual natural atomic charges before and after complexation, NPA analysis was carried out at B3LYP/6-311g (d)+LANL2DZ level of theory and the obtained results were presented in Table 3. From Table 3, it is inferred that the coordination of metal ions with the CHL has induced delocalization of charges between the ligand atoms and the central metal ions. Because of these charge transfer interactions, the positive charge on the metal ion is significantly reduced. The charge of the metal ions after complexation was 0.61, 0.89, and 0.98 e for Ag^{1+}, Ag^{2+}, and Ag^{3+}, 1.58 e for As^{5+}, 1.45 e for Cd^{2+}, 0.99, 1.05, and

0.99e for Cr^{4+}, Cr^{5+}, and Cr^{6+}, 1.38 e for Hg^{2+}, 1.41, and 1.49 e for Pb^{2+}, and Pb^{4+}, 1.08 for Se^{6+}, and 0.92 e for Tl^{3+} complexes respectively. From the obtained results, it is inferred that Cr^{6+} and Se^{6+} ions gained more amount of charges and amount of positive charge that was neutralized was found to be 5.01 and 4.92 e respectively. Whereas, the Ag^{1+} ion gains the least amount of charge and the amount of positive charge neutralized was 0.39 e. In the case of metal ions with oxidation states 2+, 3+, 4+, and 5+, the amount of charge gained by the metal ions follows the order as Ag^{2+}(1.11 e)>Hg^{2+}(0.62 e)>Pb^{2+}(0.59 e)>Cd^{2+}(0.55 e), Tl^{3+}(2.08 e)>Ag^{3+}(2.02 e), Cr^{4+}(3.01 e)>Pb^{4+}(2.51 e) and Cr^{5+}(3.95 e)>As^{5+}(3.42 e), respectively. The variation in the neutralization of positive charges for different metal ions is because the metal ions with larger oxidation states have electron accepting ability and as the oxidation states decrease, the charge accepting ability of the metal ions also decreases. The order of charge gained by the metal ions augments well with the findings of interaction energy.

3.4 Natural bond orbital (NBO) analysis

The natural charge analysis provides information about the amount of charge transferred from the ligand atoms to the metal ions. To gain deeper insight into orbitals that are involved in the charge transfer, second-order perturbation analysis was carried out at B3LYP/6-311g (d)+LANL2DZ level of theory using NBO 3.1 implemented in the Gaussian 09 software. This analysis provides detail information about the occupancy, energy of the orbital involved and stabilization energy of the electron delocalization effects. The stabilization associated with acceptor and donor NBO is calculated using the following equation.

$$E(2) = q_i \frac{F_{ij}}{\varepsilon_i - \varepsilon_j} \tag{3}$$

where q_i is the donor orbital occupancy, ε_i and ε_j are the diagonal elements (orbital energies) and F_{ij} is the off-diagonal NBO fock matrix element. The calculated results were presented in the Supplementary Tables S1. From the obtained results, the orbital interactions of the type LP-LP*, LP-LP, and LP-BD* were observed for the CHL-M^{n+} metal complexes and implies that the electrons are delocalized from the non-bonding orbital (LP) of the ligand atoms to the non-bonding (LP), anti-non-bonding (LP*) and anti-bonding (BD*) orbital of the metal ions. On comparing the occupancies of the LP, LP* before and after metal chelation, it is inferred that there are significant changes in their respective orbital. The calculated LP orbital occupancy for the isolated CHL is found to be in the range 1.91 - 1.92. After the complex formation, the LP orbital occupancy of the ligand atoms is found to be decreased in the range of 0.05 – 1.11. Whereas in the case of metal ions, the occupancy of the LP, LP* and BD* orbital corresponding to the metal ions were found to be zero i.e. they are empty orbital. During the metal complex formation, there is delocalization of electrons from the ligand atoms to the empty orbital of the metal ions. As a result of this, occupancies corresponding to the LP, LP* and BD*

orbital of the metal ions are found to be increased in the range 0.05 – 1.45. The occupancies of the metal ions with higher oxidation states such as 6+, 5+, 4+, and 3+ possess the higher orbital occupancies whereas, the metal ions with 2+ oxidation state possess lower orbital occupancies. This is due to the fact the metal ions with higher oxidation states possess higher electron withdrawing ability rather than the metal ions with lower oxidation states.

3.5 QTAIM analysis

Table 4. Topological parameters (electron density ρ(r), Laplacian of electron density ∇2ρ(r), and total electron density HBCP(r)) corresponding to the coordination bonds of the CHL-Mn+ metal complexes calculated at B3LYP/6-311g (d)+LANL2DZ level of theory.

Complexes	N6-M^{n+}			N7-M^{n+}			N8-M^{n+}			N9-M^{n+}		
	ρ(r)	$\nabla^2\rho(r)$	$H_{BCP}(r)$	ρ(r)	$\nabla^2\rho(r)$	$H_{BCP}(r)$	ρ(r)	$\nabla^2\rho(r)$	$H_{BCP}(r)$	ρ(r)	$\nabla^2\rho(r)$	$H_{BCP}(r)$
CHL-Ag^{1+}	0.067	0.305	-0.011	0.048	0.213	-0.004	0.068	0.305	-0.012	0.053	0.239	-0.006
CHL-Ag^{2+}	0.098	0.394	-0.026	0.077	0.306	-0.016	0.096	0.386	-0.025	0.087	0.342	-0.021
CHL-Ag^{3+}	0.105	0.365	-0.030	0.087	0.301	-0.021	0.101	0.355	-0.028	0.097	0.324	-0.026
CHL-As^{5+}	0.095	0.355	-0.032	0.050	0.054	-0.011	0.076	-0.188	-0.071	0.074	-0.199	-0.072
CHL-Cd^{2+}	0.076	0.326	-0.020	0.060	0.257	-0.010	0.077	0.322	-0.020	0.067	0.287	-0.014
CHL-Cr^{4+}	0.093	0.388	-0.025	0.070	0.303	-0.013	0.087	0.374	-0.022	0.085	0.350	-0.021
CHL-Cr^{5+}	0.094	0.367	-0.027	0.068	0.283	-0.012	0.088	0.352	-0.023	0.085	0.328	-0.021
CHL-Cr^{6+}	0.100	0.386	-0.031	0.070	0.285	-0.014	0.092	0.364	-0.026	0.095	0.348	-0.028
CHL-Hg^{2+}	0.075	0.276	-0.018	0.057	0.211	-0.010	0.075	0.272	-0.018	0.064	0.240	-0.013
CHL-Pb^{2+}	0.034	-0.063	-0.022	0.032	-0.021	-0.015	0.034	-0.063	-0.022	0.033	-0.061	-0.021
CHL-Pb^{4+}	0.034	-0.064	-0.022	0.031	-0.014	-0.013	0.034	-0.066	-0.022	0.033	-0.063	-0.021
CHL-Se^{6+}	0.092	0.049	-0.043	0.063	0.117	-0.013	0.086	0.088	-0.034	0.100	-0.013	-0.056
CHL-Tl^{3+}	0.036	0.106	-0.004	0.028	0.083	-0.001	0.039	0.110	-0.005	0.034	0.100	-0.004

The QTAIM analysis is an intuitive tool that provides information about the electron density ρ(r), Laplacian of electron density $\nabla^2\rho(r)$, and total electron density ($H_{BCP}(r) = G_{BCP}(r) + V_{BCP}(r)$) at the BCP corresponding to the metal-ligand bonds such as N6-M^{n+}, N7-M^{n+}, N8-M^{n+}, and N9-M^{n+} respectively. The values of ρ(r) describes the strength of the metal-ligand bond and sign of the $\nabla^2\rho(r)$, and $H_{BCP}(r)$ values describes whether the electron is locally concentrated ($\nabla^2\rho(r) < 0$; $H_{BCP}(r) < 0$ indicates covalent interactions) or depleted ($\nabla^2\rho(r) > 0$; $H_{BCP}(r) > 0$ indicates non-covalent interactions such as hydrogen bond, ionic bond, and van der Waals interaction) and nature of the metal-ligand interactions. The calculated values respective of the ρ(r), $\nabla^2\rho(r)$,

and $H_{BCP}(r)$ at BCP for the CHL-M^{n+} complexes are summarized in Table 4. The range of $\rho(r)$ for the N-M^{n+} bonds are found to be 0.048 – 0.105 a.u for CHL-Ag^{n+} (where n = 1, 2, and 3), 0.054 – 0.095 a.u for As^{5+}, 0.060 – 0.077 a.u for Cd^{2+}, 0.068 – 0.100 a.u CHL-Cr^{n+} (where n = 4, 5, and 6), 0.057 – 0.075 a.u for CHL-Hg^{2+}, 0.031 - 0.034 a.u for CHL-Pb^{n+} (where n = 2, and 4), 0.063 – 0.100 a.u for Se^{6+}, 0.028 - 0.039 a.u for CHL-Tl^{3+} complexes respectively. It is inferred that the bonds with higher electron density possess shortest bond distance and vice versa as seen in the cases of CHL-Pb^{2+}, CHL-Pb^{4+}, and CHL-Tl^{3+} complexes which possess minimum electron density and it is evident from the larger bond distance. Whereas, CHL-Ag^{3+} and CHL-Cr^{n+} complexes possess the maximum electron density and it is evident from the shorter bond distance. Moreover, the negative value of $\nabla^2\rho(r)$ and $H_{BCP}(r)$ along with least $\rho(r)$ observed for the CHL-Pb^{2+} and CHL-Pb^{4+} complexes implies that the nature of the interaction between the metal and ligand is found to be weak covalent interactions. While for the remaining complexes the positive values of $\nabla^2\rho(r)$ and negative values of $H_{BCP}(r)$ were observed. This implies that the interaction between the metal and ligands are partially covalent and partially ionic in nature.

4. Conclusions

This study provides a comprehensive analysis of the chelation of heavy metal ions by the chlorophyll molecule. Our investigation has shown that chlorophyll can form stable complexes with a variety of heavy metals, including Ag^{1+}, Ag^{2+}, Ag^{3+}, As^{5+}, Cd^{2+}, Cr^{4+}, Cr^{5+}, Cr^{6+}, Hg^{2+}, Pb^{2+}, Pb^{4+}, Se^{6+}, and Tl^{3+}. The geometry of these complexes varies, with CHL-Ag^{2+}, CHL-Cr^{4+}, CHL-Cr^{5+}, CHL-Cr^{6+}, and CHL-Se^{6+} exhibiting nearly square planar structures, while CHL-Ag^{1+}, CHL-Ag^{3+}, CHL-As^{5+}, CHL-Cd^{2+}, CHL-Hg^{2+}, CHL-Pb^{2+}, CHL-Pb^{4+}, and CHL-Tl^{3+} demonstrate square-pyramidal-like geometry.

The affinity of heavy metals for chlorophyll follows a specific order, with CHL-Cr^{6+} showing the highest affinity and CHL-Ag^{1+} the lowest. The NPA and NBO analyses indicate that heavy metals accept electrons from the ligand atoms, resulting in reduced positive charges on the metal ions. QTAIM analysis further reveals that the nature of metal-ligand bonding ranges from weakly covalent to a mix of covalent and ionic interactions.

These findings suggest that chlorophyll is an effective natural chelating agent, capable of binding and immobilizing a wide range of heavy metals. This ability highlights its potential application in detoxifying heavy metals from the human body and the environment. Future research should explore the practical applications of chlorophyll-based chelation in environmental remediation and medical treatments for heavy metal poisoning.

References

[1] M. Balali-Mood, K. Naseri, Z. Tahergorabi, M.R. Khazdair, M. Sadeghi, Toxic Mechanisms of Five Heavy Metals: Mercury, Lead, Chromium, Cadmium, and Arsenic,

Frontiers in Pharmacology, 12, (2021) 643972. https://doi.org/10.3389/fphar.2021.643972

[2] A.S. Prasad, Zinc in human health: Effect of zinc on immune cells. Molecular Medicine, 14, (2008) 353-357. https://doi.org/10.2119/2008-00033.Prasad

[3] M.C. Linder, (1991) Biochemistry of Copper, Plasma Protein Turnover 120, 125-131. https://doi.org/10.1007/978-1-4757-9432-8

[4] A.T. Jan, M. Azam, K. Siddiqui, A. Ali, I. Choi, Q.M. Haq, Heavy Metals and Human Health: Mechanistic Insight into Toxicity and Counter Defense System of Antioxidants. International Journal of Molecular Sciences, 16(12), (2015) 29592-29630. https://doi.org/10.3390/ijms161226183

[5] J. Briffa, E. Sinagra, R. Blundell, Heavy metal pollution in the environment and their toxicological effects on humans, Heliyon 6, (2020) e04691. https://doi.org/10.1016/j.heliyon.2020.e04691

[6] G.A. Engwa, P.U. Ferdinand, F. N. Nwalo, M.N. Unachukwu, (2019) Mechanism and Health Effects of Heavy Metal Toxicity in Humans. IntechOpen. https://doi.org/10.5772/intechopen.82511

[7] L. Patrick, Lead toxicity, a review of the literature. Part I: Exposure, evaluation, and treatment. Alternative Medicine Review, 11(1), (2006) 2-22.

[8] T.W. Clarkson, L. Magos, G. J. Myers, The toxicology of mercury - Current exposures and clinical manifestations. New England Journal of Medicine, 349, (2003) 1731-1737. https://doi.org/10.1056/NEJMra022471

[9] S. Satarug, S.H. Garrett, M.A. Sens, D.A. Sens, Cadmium, environmental exposure, and health outcomes, Environmental Health Perspectives, 118, (2010) 182-190. https://doi.org/10.1289/ehp.0901234

[10] M.F. Hughes, B.D. Beck, Y. Chen, A.S. Lewis, Arsenic exposure and toxicology: A historical perspective, Toxicological Sciences, 123(2), (2011) 305-332. https://doi.org/10.1093/toxsci/kfr184

[11] B. J. Alloway, (Ed.), (2013). Heavy Metals in Soils: Trace Metals and Metalloids in Soils and their Bioavailability. 4th ed. Springer. https://doi.org/10.1007/978-94-007-4470-7

[12] G. Sposito, (2008) The Chemistry of Soils. 2nd ed. Oxford University Press.

[13] N.A.A. Qasem, R.H. Mohammed, D.U. Lawal, Removal of heavy metal ions from wastewater: a comprehensive and critical review, npj Clean Water, 4, 36 (2021). https://doi.org/10.1038/s41545-021-00127-0

[14] X. Shen, M. Dai, J. Yang, L. Sun, X. Tan, C. Peng, I. Ali, I. Naz, A critical review on the phytoremediation of heavy metals from environment: Performance and challenges. Chemosphere, 291(3), (2022) 132979. https://doi.org/10.1016/j.chemosphere.2021.132979

[15] M. Knapp, J. Bridwell-Rabb, The green pigment of life, Nature Chemistry, 14, (2022) 1202. https://doi.org/10.1038/s41557-022-01052-6

[16] K. Zhdanova, M. Ivantsova, M. Vyal'ba, K. Usachev, S. Gradova, S. Градов, S. Karpechenko, N. Bragina, Design of A3B-Porphyrin conjugates with terpyridine as potential theranostic agents: Synthesis, complexation with Fe(III), Gd(III), and

photodynamic activity. Pharmaceutics, 15(1), (2023), 269-269. https://doi.org/10.3390/pharmaceutics15010269

[17] F. Schmitt, P. Govindaswamy, G. Süß-Fink, W. H. Ang, P. J. Dyson, L. Juillerat-Jeanneret, B. Therrien, Ruthenium porphyrin compounds for photodynamic therapy of cancer, Journal of Medicinal Chemistry, 51(6), (2008), 1811-1816. https://doi.org/10.1021/jm701382p

[18] H. Huang, W. Song, J. Rieffel, J.F. Lovell, Emerging Applications of Porphyrins in Photomedicine. Frontiers in Physics, 3, (2015). https://doi.org/10.3389/fphy.2015.00023

[19] A.D. Becke, Density-functional thermochemistry. III. The role of exact exchange, Journal of Chemical Physics, 98 (1993) 5648-5652. https://doi.org/10.1063/1.464913

[20] C. Lee, W. Yang, R.G. Parr, Development of the Colle-Salvetti correlation-energy formula into a functional of the electron density, Physical Review B, 37, (1988) 785-789. https://doi.org/10.1103/PhysRevB.37.785

[21] P.J. Hay, W.R. Wadt, Ab initio effective core potentials for molecular calculations. Potentials for the transition metal atoms Sc to Hg, Journal of Chemical Physics, 82, (1985) 270-283. https://doi.org/10.1063/1.448799

[22] P.J. Hay, W.R. Wadt, Ab initio effective core potentials for molecular calculations. Potentials for K to Au including the outermost core orbitals, Journal of Chemical Physics, 82 (1985) 299-310. https://doi.org/10.1063/1.44879

[23] P.J. Hay, W.R. Wadt, Ab initio effective core potentials for molecular calculations. Potentials for main group elements Na to Bi, Journal of Chemical Physics, 82 (1985), 284-298. https://doi.org/10.1063/1.448800

[24] S.F. Boys, F. de Bernardi, The calculation of small molecular interactions by the differences of separate total energies. Some procedures with reduced errors, Molecular Physics, 19 (1970), 553-566. https://doi.org/10.1080/00268977000101561

[25] R. Shankar, P. Kolandaivel, L. Senthilkumar, Interaction studies of cysteine with Li^+, Na^+, K^+, $Be2^+$, $Mg2^+$, and $Ca2^+$ metal cation complexes, Journal of Physical Organic Chemistry, 24 (2011), 553-567. https://doi.org/10.1002/poc.1786

[26] C. Pitchumani Violet Mary, S. Vijayakumar, R. Shankar, Metal chelating ability and antioxidant properties of Curcumin-metal complexes - A DFT approach, Journal of Molecular Graphics and Modelling, 79, (2018) 1-14. https://doi.org/10.1016/j.jmgm.2017.10.022

[27] C. Pitchumani Violet Mary, R. Shankar, S. Vijayakumar, P. Kolandaivel, Interaction studies of human prion protein (HuPrP109-111: methionine-lysine-histidine) tripeptide model with transition metal cations, Journal of Molecular Graphics and Modelling, 69, (2016) 111-126. https://doi.org/10.1016/j.jmgm.2016.08.012

[28] A.E. Reed, R.B. Weinstock, F. Weinhold, Natural population analysis, Journal of Chemical Physics, 83, (1985) 735-746. https://doi.org/10.1063/1.449486

[29] E.D. Glendening, A.E. Reed, J.E. Carpenter, F. Weinhold, (1990) NBO 3.0 Program Manual. Theoretical Chemistry Institute, University of Wisconsin, Madison, WI.

[30] R.F.W. Bader, (1990) Atoms in Molecules, A Quantum Theory, Oxford Science Publications, Clarendon Press, London. https://doi.org/10.1093/oso/9780198551683.001.0001

[31] T. Lu, F. Chen, Multiwfn : A Multifunctional Wavefunction Analyzer, Journal of Computational Chemistry, 33, (2012) 580-592. https://doi.org/10.1002/jcc.22885

[32] M.J. Frisch, G.W. Trucks, H.B. Schlegel, G.E. Scuseria, M.A. Robb, J.R. Cheeseman, (2010)Gaussian 09 Revision B.01.Gaussian, Inc., Wallingford CT.

Conflict of interest: The Authors have no conflicts of interest to declare that they are relevant to the content of this article.